Veterinary Microbiology 234 (2019) 51–60

Contents lists available at ScienceDirect

Veterinary Microbiology

journal homepage: www.elsevier.com/locate/vetmic

FUNDC1-mediated mitophagy in bovine papillomavirus-infected urothelial cells

Sante Roperto[a,*], Valeria Russo[a], Francesca De Falco[a], Alessandra Rosati[b], Cornel Catoi[c], Franco Roperto[d]

[a] Dipartimento di Medicina Veterinaria e Produzioni Animali, Università di Napoli Federico II, Napoli, Italy
[b] Dipartimento di Medicina Chirurgia ed Odontoiatria, Schola Medica Salernitana, Università di Salerno, Baronissi, Italy
[c] University of Agricultural Sciences and Veterinary Medicine, Faculty of Veterinary Medicine, Pathology Department, Cluj-Napoca, Romania
[d] Dipartimento di Biologia, Università di Napoli Federico II, Napoli, Italy

ARTICLE INFO

Keywords:
BPV E5 oncoprotein
FUNDC1
Receptor mitophagy
DRP1
Bag3
DRP1 receptors

ABSTRACT

E5 protein, the major oncoprotein of the bovine *Deltapapillomavirus* genus, has been detected in 17 of the 19 urothelial cancers by molecular and morphological procedures. In 10 urothelial cancers, the oxygen sensitive subunit HIF-1α, which is upregulated by hypoxia, was overexpressed. Mitophagy, the selective autophagic removal of dysfunctional mitochondria, was upregulated in hypoxic neoplastic cells infected by BPVs which was mediated by FUNDC1, a mitochondrial outer-membrane protein. The FUNDC1 receptor was amplified by PCR, and amplicon sequencing showed a 100% homology with bovine FUNDC1 sequences deposited in GenBank (accession number: NM_001104982). Both transcripts and protein levels of FUNDC1 were significantly decreased in hypoxic neoplastic cells relative to healthy, non-neoplastic cells. FUNDC1 interacted with the LC3 protein, a marker of autophagosome (mitophagosome) membrane, the Hsc70/Hsp70 chaperone, and Bag3 co-chaperone. Bag3 may play a role in mitophagosome formation together with the Synpo2 protein, and may be involved in the degradation of Hsc70/Hsp70-bound CHIP-ubiquitinated cargoes, in association with its chaperone. Ultrastructural findings revealed the presence of mitochondria exhibiting severe fragmentation and loss of cristae, as well as numerous mitochondria-containing autophagosomes. Total and phosphorylated GTPase dynamin-related protein 1 (DRP1), which plays a crucial role in mitochondrial fission, a pre-requisite for mitophagy, was overexpressed at the mitochondrial level. Total and phosphorylated mitochondrial fission factor (Mff), mitochondrial fission protein 1 (Fis1), mitochondrial dynamics 51 (MiD51), and MiD49, which are DRP1 receptors responsible and/or co-responsible for its mitochondrial recruitment were overexpressed.

1. Introduction

Mitophagy is a selective form of autophagy, specific to the degradation of dysfunctional mitochondria. It is a fundamental process that plays a crucial role in maintaining a healthy and functional mitochondrial network, and, consequently, mediating cell survival and viability in response to infection (Youle and Narendra, 2011). Mitophagy and mitochondrial dynamics, which refers to the repetitive cycle of fusion and fission between mitochondria, determine the mitochondrial homeostasis and influence nearly every aspect of mitochondrial function (Twig and Shirihai, 2011). While it is known that the mitochondrial dynamics are linked to mitophagy (Hamacher-Brady and Brady, 2016), the detailed mechanisms of the interplay between mitochondrial dynamics and mitophagy remain poorly understood (Chen et al., 2016).

In mammalian cells, mitophagy is triggered by a variety of cellular events (Pickles et al., 2018). The mechanisms of mitophagy can be classified in two groups, i.e. Parkin-dependent and Parkin-independent mitophagy (Youle and Narendra, 2011; Zhang et al., 2018), the latter being mediated by receptors such as NIX (BNIP3-like protein X), BNIP3 (BCL2 interacting protein 3) and FUNDC1 (FUN14 domain containing protein 1), which are prevalently localised to the outer mitochondrial membrane (OMM) (Rodger et al., 2018). One common feature of mitophagy receptors is that they harbour an LC3-interacting region (LIR), thus, promoting the sequestration of mitochondria into the isolation membrane (Liu et al., 2012).

FUNDC1, encoded by a gene located on chromosome X, is highly conserved from *Drosophila* to humans (Liu et al., 2012). FUNDC1 is

* Corresponding author.
E-mail address: sante.roperto@unina.it (S. Roperto).

https://doi.org/10.1016/j.vetmic.2019.05.017
Received 26 March 2019; Received in revised form 22 May 2019; Accepted 22 May 2019

known to regulate mitochondrial dynamics and Parkin-independent hypoxia-induced mitophagy (Liu et al., 2014; Chen et al., 2016). Indeed, FUNDC1 interacts with LC3 through its LIR motif under hypoxic conditions, and plays crucial roles in autophagosome formation and target recognition (Liu et al., 2012). Recently, a new role of FUNDC1 has been suggested in response to proteotoxic stresses, thus, promoting cellular proteostasis via its interaction with cytosolic Hsc70/Hsp70 (Li et al., 2019). FUNDC1 plays a central role in mitochondrial fission, which is a prerequisite for mitophagy (Twig and Shirihai, 2011).

Hypoxia-induced FUNDC1-mediated mitophagy was discovered only recently (Liu et al., 2012). Mammalian mitophagy in vivo is emerging as more complex than previously thought; however, recent breakthroughs have been achieved from in vivo studies using transgenic mice, showing that mitophagy is different between and within tissues (Sun et al., 2015; Palikaras et al., 2018).

Bovine papillomaviruses (BPVs) comprise 25 types classified into five genera (https://pave.niaid.nih.gov/; Ling et al., 2019). The Deltapapillomavirus (δPV) genus is composed of four high-risk members, namely BPV-1, BPV-2, BPV-13, and BPV-14 (Daudt et al., 2018). Bovine δPVs are responsible for both abortive infections through E proteins, resulting in transformation of cells, and for productive infections, leading to virus replication in epithelial as well as non-epithelial cells (Roperto et al., 2011, 2012; Roperto et al., 2013a).

In southern Italy, BPV-2 and BPV-13 are the most important infectious agents associated with urothelial tumours, found very commonly in some breeds of pasture-residing cattle that graze on bracken fern-infested lands (Roperto et al., 2016). Bovine δPVs exhibit their transforming activity through the E5 protein, which is the most highly conserved oncoprotein (DiMaio and Petti, 2013). Numerous molecular pathways have been identified through which E5 oncoprotein is responsible for cellular transformation of naturally occurring urothelial tumours. It binds to the activated form of platelet-derived growth factor ß receptor (PDGFßR) (Roperto et al., 2013b). E5 has been shown to display transforming activity via calpain3 pathway, which is proteolytically active in urothelial cancer cells (Roperto et al., 2010b). In addition, E5 binds to the D subunit of the V_1-ATPase proton pump (Roperto et al., 2014). E6 and E7 are less studied δPV oncoproteins.

The aim of the present paper was to report a mechanistic study about molecular and ultrastructural findings that characterise the FUNDC1-mediated mitophagy in bovine PV-infected urothelial cells.

2. Materials and methods

2.1. Ethics statement

In this study, we did not perform any animal experiments. All the samples were collected post-mortem from slaughterhouses, and therefore, no ethics approval is required.

2.2. Tumour samples

Urothelial samples from 19 cows suffering from clinical chronic enzootic haematuria were collected from public slaughterhouses after bladder neoplasms had been identified during routine meat inspection. Additional 15 mucosa samples of urinary bladder were also collected from apparently healthy cows. Both neoplastic and non-neoplastic bladder samples were subdivided and either fixed in 10% buffered formalin for microscopic investigation or immediately frozen in liquid nitrogen and stored at −80 °C for subsequent molecular biological analysis.

2.3. Histopathology

The tissues were processed routinely for paraffin embedding. Histological diagnosis was carried out using 5-µm-thick haematoxylin-eosin (HE)–stained sections based on previously suggested morphological criteria (Roperto et al., 2010a).

2.4. Transmission electron microscopy (TEM)

Non-neoplastic and neoplastic bladder samples were immediately fixed in 4% glutaraldehyde in 0.1 M phosphate buffer (pH 7.4) for 2–3 h. Postfixation was performed with 1% osmium tetroxide (OsO_4) in the same buffer for 1 h. They were washed again in 0.1 M phosphate buffer (pH 7.4) and then dehydrated using graded alcohol series, following which, they were embedded in Agar Low Viscosity Resin (AGR 1078) (Agar Scientific Limited, Essex, England). Semi-thin sections (400 nm) were cut with a glass knife on an EM UC6 ultramicrotome (Leica Microsystems) and stained with 1% toluidine blue. Ultra-thin sections (60–70 nm) were obtained using the same ultramicrotome with a diamond knife and collected onto 300-mesh copper grids coated with formvar. Counterstaining was performed with lead citrate and uranyl acetate. The sections were observed using a JEOL JEM-1011 transmission electron microscope (JEOL, Tokyo, Japan) equipped with a thermionic tungsten filament at an acceleration voltage of 100 kV. Images were taken using a Morada cooled slow-scan CCD camera (3783 × 2672 pixels) and micrographs were taken with iTEM software (Olympus Soft Imaging System GmbH, Munster, Germany).

2.5. Antibodies

Rabbit antibody against FUNDC1 was obtained from Aviva Systems Biology (CA, USA); rabbit antibodies against DRP1, pDRP1, Mff and pMff were from Cell Signaling (LID, NL); mouse antibodies against MID49, MID51, Fis1, Hsc70/Hsp70, CHIP, and β-actin were from Santa Cruz Biotechnology (TX, USA); rabbit antibodies against LC3 and HIF-1α were from Novus Biologicals (CO, USA); rabbit antibody against Synpo2 was from Biorbyt (CA, USA); rabbit antibody against Bag3 was from Biouniversa (AV, IT); rabbit polyclonal antiserum against E5 (recognizing the C-terminal 14 amino acids of the BPV E5 protein) was kindly provided by Prof. DiMaio, Yale University, New Haven, USA.

2.6. RNA extraction and reverse transcription (RT)-PCR

Total RNA was extracted from 19 bovine urothelial tumour samples and 15 bladder samples from healthy cows using an RNeasy Mini Kit (Qiagen TM, ME, DE), in accordance with the manufacturer's instructions. Genomic DNA was removed from the RNA preparations using RNase-free DNase I from Fermentas Life Sciences (Thermo Fisher Scientific, MA, USA). A 1-µg sample of the total RNA was used to generate the single strand of cDNA by the QuantiTect Reverse Transcription Kit (Qiagen TM, ME, DE), according to the manufacturer's instructions. PCR was performed with a specific primer set designed by the Primer3 online tool for E5 gene of BPV-2, BPV-13, and FUNDC1. The following primers were used: BPV-2 E5 ORF forward 5′-CACTGC CATTTGTTTTTTTC-3′, reverse 5′-GGAGCACTCAAAATGATCCC-3′; BPV-13 E5 ORF forward 5′-CACTGCCATTTGGTGTTCTT-3′, reverse 5′-AGCAGTCAAAATGATCCCAA-3′; FUNDC1 forward 5′- CGGTAGCCACC CAGATTGTAA-3′; reverse 5′-AC TGGCAATCTGAAGGAGAAGA-3′. The PCR conditions were: 94 °C for 5 min, 40 cycles of 95 °C for 30 s, 56 °C for 30 s, and 72 °C for 30 s.

2.7. Sequence analysis

PCR products, obtained by RT-PCR, were purified by Qiaquick PCR purification Kit (Qiagen TM, ME, DE) and bidirectionally sequenced using a BigDye_Terminator v1.1 Cycle Sequencing Kit (Applied Biosystems, CA, USA), following manufacturer's recommendations. The sequences were dye-terminator removed by DyeEx 2.0 spin kit (Qiagen TM, ME, DE) and run on a 3500 Genetic Analyser (Applied Biosystems, CA, USA). Electropherograms were analysed using Sequencing analysis v5.2 and sequence scanner v1.0 software (Applied Biosystems, CA,

USA). The sequences obtained were analysed by BLAST program.

2.8. Real time RT-PCR

To perform real time RT- PCR analysis, total RNA and cDNA from 19 bovine urinary bladder tumour and 15 normal urothelium samples were generated as reported above. Real time PCR was carried out on a Bio Rad CFX Connect™ Real Time PCR Detection System (Bio Rad Hercules, CA, USA) using iTAq Universal SYBR® Green Supermix (Bio Rad Hercules, CA, USA). Each reaction was set in triplicate and the primers used for FUNDC1 were the same as that for RT-PCR. The thermal profile for the PCR was: 95 °C for 10 min, 40 cycles of 94 °C for 15 s, 56 °C for 30 s, followed by a melting curve. The relative quantification (RQ) was carried out using CFX Manager™ software, based on the equation $RQ = 2^{-\Delta\Delta Cq}$, where Cq is the quantification cycle to detect fluorescence. Cq data were normalised to the reference β-actin gene (forward: 5′- TAGCACAGGCCTCTCGCCTTCGT-3′, reverse 5′-GCACATGCCGGAG CCGTTGT-3′).

2.9. Statistical analysis

Results are presented as means ± SE. The expression levels were assessed by one-way ANOVA, followed by Tukey's test for multiple comparisons of means, using GraphPad PRISM software version 8 (GraphPad Software, San Diego, CA). P values ≤ 0.05 were considered statistically significant.

2.10. Western blot analysis

Healthy and neoplastic bovine urothelial samples were lysed in RIPA buffer (50 mM Tris-HCl pH 7.5, 1% Triton X-100, 400 mM NaCl, 1 mM EDTA, 2 mM PMSF, 1.7 mg/ml Aprotinin, 50 mM NaF, and 1 mM sodium orthovanadate). The protein concentration was measured using the Bradford assay (Bio-Rad, CA,USA). For western blotting, 50 µg of lysate proteins were heated a 90 °C in 4× premixed Laemmli sample buffer (Bio-Rad, CA, USA). They were clarified by centrifugation, separated by SDS-PAGE, and transferred onto nitrocellulose membranes (GE Healthcare, UK, RPN303D). The membranes were blocked with TBST (TBS and 0.1% Tween 20) containing 5% no- fat dry milk for 1 h at room temperature, and subsequently incubated overnight at 4 °C with primary antibodies before being listed. The membranes were washed thrice with TBST, incubated for 1 h at room temperature with goat anti-rabbit (Bio-Rad, CA, USA) and goat anti-mouse (Bio-Rad, CA, USA) HRP-conjugated secondary antibodies diluted at 1:2000 in TBST, and washed thrice with TBST. Immunoreactive bands were detected using Western Blotting Luminol Reagent (Santa Cruz Biotechnology, TX, USA) and ChemiDoc XRS Plus (Bio-Rad, CA, USA). Images were acquired with Image Lab Software version 2.0.1.

2.11. Cell fractionation and mitochondria isolation

Mitochondria from 10 bovine urothelial tumour samples and 6 bladder samples from healthy cows were prepared using the Qproteome mitochondria isolation kit (Qiagen TM, ME, DE). Briefly, 60 mg slices were cut from each tissue examined, washed in 0.9% NaCl, and incubated for 10 min at 4 °C in lysis buffer. The homogenate was centrifuged at 1000xg for 10 min at 4 °C, and the supernatant was designated as the cytosolic fraction. The pellet was resuspended in disruption buffer and passed through a 26-gauge needle 15 times. Enriched nuclei fraction was pelleted by centrifugation at 1000 x g for 10 min and homogenised in a disruption buffer. To obtain the enriched mitochondrial fraction, the supernatant was centrifuged at 6000xg for 10 min at 4 °C. The pellet contained the mitochondria and the supernatant constituted the microsomal fraction. The pellet was resuspended in mitochondria storage buffer. All buffers, except mitochondria storage buffer, were supplemented with protease inhibitors at 1:100, provided within the kit. Protein concentration in the different fractions was determined with Bio-Rad protein assay (Bio-Rad, CA, USA).

2.12. Mitochondria immunoprecipitation

Mitochondrial extracts from normal and pathological bladders, obtained as previously described, were immunoprecipitated. Protein samples (100 µg) were incubated with anti-FUNDC1 or anti-BAG-3 primary antibodies for 1 h at 4 °C with gentle shaking. Following the incubation, centrifugation (1,000xg, 5 min at 4 °C) was carried out, and the samples were collected and incubated overnight with 30 µl of Protein A/G-Plus Agarose (sc-2003) (Santa Cruz Biotechnology, TX, USA) at 4 °C. Immunoprecipitates were washed four times in complete lysis buffer (as described above), and separated on polyacrylamide gels. Following the transfer of proteins, membranes were blocked for 1 h at room temperature in 5% bovine serum albumin, and incubated overnight with respective primary antibodies at 4 °C. After three washes in Tris-buffered saline, membranes were incubated with the respective secondary antibodies for 1 h at room temperature. Chemiluminescent signals were then developed with Western Blotting Luminol Reagent (Santa Cruz Biotechnology, TX, USA), and detected by the ChemiDoc XRS Plus gel documentation system (Bio-Rad, CA, USA).

3. Results

3.1. Microscopic patterns and virological findings

Ten of the nineteen tumors were diagnosed as papillary carcinomas (7 high-grade and 3 low-grade); two as papillary urothelial neoplasms of low malignant potential (PUNLMPs); five were invasive carcinomas (3 high-grade and 2 low-grade) and two were consistent with carcinoma in situ (CIS) (Supplemental Table S1). Virological findings were characterised by the expression of BPV-2 and BPV-13 as unveiled through detection of E5 transcripts by RT-PCR composed of 154 and 153bp, respectively (Supplemental Fig. S1). E5 oncoprotein was also detected by western blot (Supplemental Fig. S1). Neither BPV E5 transcripts nor E5 oncoprotein expression were detected in any of the non-neoplastic bladder samples.

3.2. Abnormal mitochondrial dynamics-associated mitophagy induced by hypoxia

Fragmentation and loss of mitochondrial cristae were the peculiar ultrastructural characteristics of urothelial cancer cells infected by BPVs. Furthermore, submicroscopic findings consistent with the presence of pre-autophagosomal structures (PAS) or phagophores were also observed (Fig. 1). These concomitant ultrastructural features suggested that the mitochondrial dynamics were altered, and a selective removal of damaged mitochondria (mitophagy) may build up in these cells.

Emerging evidence suggests that various signalling pathways converge on autophagy in response to hypoxia in cancer cells (Daskalaki et al., 2018). Furthermore, an extensive fragmentation of mitochondria leading to mitophagy is induced by hypoxia, a very common feature of tumour cells. Therefore, we first wanted to test whether urothelial cancer cells infected by BPVs were actually under hypoxic conditions, similar to the epithelial cells infected by HPVs (Guo et al., 2014). Western blot analysis performed on healthy and neoplastic urothelial cells showed statistically significant overexpression of HIF-1α protein levels in neoplastic cells (Fig. 2), indicating that urothelial cancer cells are under hypoxic stress as HIF-1α is an oxygen-sensitive subunit and its expression is induced by hypoxia (Masoud and Li, 2015).

As hypoxia is known to induce mitophagy mediated by receptors (Liu et al., 2012), we investigated the expression of the highly conserved FUNDC1 receptor, an integral mitochondrial outer-membrane 155 amino acid protein, which controls both mitochondrial dynamics

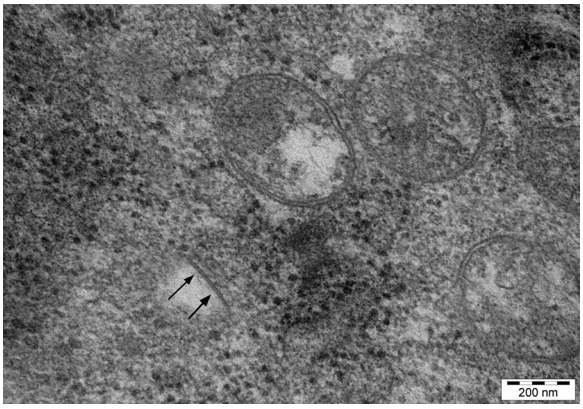

Fig. 1. Severe fragmentation and loss of mitochondrial cristae are shown. Ultrastructural features consistent with the presence of phagophore membrane are seen (arrow).

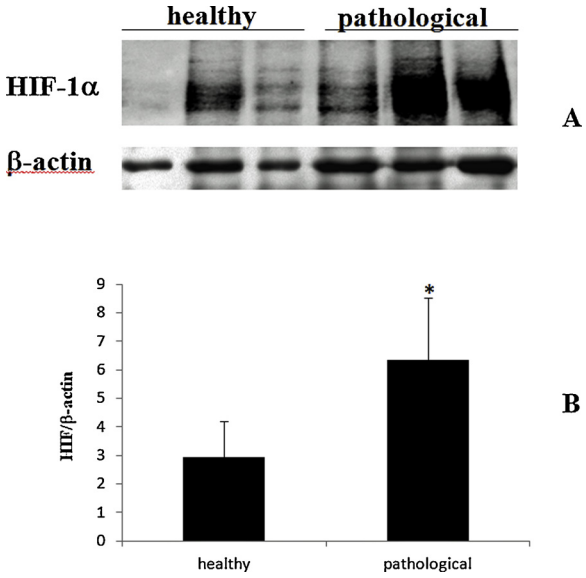

Fig. 2. (A): HIF-1α western blot analysis for healthy and neoplastic urothelial cells. Lanes 1–3: bladder samples from healthy cows; lanes 4–6: three representative papillary urothelial cancers. (B): the lower part of the western blot showed a densitometric analysis. Statistically significant overexpression of HIF-1α protein levels was indicated in neoplastic cells (* $p < 0.05$).

and mitophagy under hypoxic conditions (Wu et al., 2016). First, we wanted to investigate if FUNDC1 is constitutively expressed in bovine urothelial cells. Therefore, we performed RT-PCR analysis and detected 125 bp transcript sequences, the alignment of which showed a 100% identity with bovine FUNDC1 deposited in GenBank (accession number: NM_001104982) (Fig. 3).

As it has been suggested that both mRNA and protein levels of FUNDC1 are reduced in response to hypoxia (Liu et al., 2012), we investigated this using real time RT-PCR analysis of FUNDC1 mRNA, and found a reduction in its levels in 6 out of the 19 neoplastic samples (˜32%) (Fig. 4). As post-translational changes are known to occur (Liu et al., 2014), we also carried out western blot analysis for FUNDC1 protein in total extracts which was reduced in further 4 neoplastic samples with normal mRNA levels (Fig. 4). Taken together, FUNDC1 mRNA and protein levels were downregulated in 10 out of the 19 neoplastic samples (˜53%). Furthermore, we carried out western blot analysis for mitochondrial, cytosolic, and microsomal fractions, and FUNDC1 was localised mostly in the mitochondrial fraction. The FUNDC1 protein was just barely detectable in microsomal and cytosolic fractions of both healthy and neoplastic cells, thus, confirming that FUNDC1 protein is preferentially localised on mitochondria under chronic hypoxia. FUNDC1 of the mitochondrial fraction appeared to have a reduced expression in neoplastic cells infected by BPVs, in comparison with healthy non-neoplastic cells (Fig. 5).

It has been shown that FUNDC1 interacts, through its LIR, with LC3, an autophagy-related protein that is essential for autophagosome biogenesis, and that this interaction is enhanced by hypoxia (Liu et al., 2012). To explore whether this interaction takes place in naturally occurring papillomavirus infections, we performed western blot analysis on mitochondrial fractions immunoprecipitated by an anti-FUNDC1 antibody, and detected the presence of LC3 protein, which demonstrates that FUNDC1 is physically associated with LC3, the lipidated component of which (LC3B), is overexpressed in urothelial cells infected by BPVs (Roperto et al., 2018). This mechanistic interaction was more evident in neoplastic than in healthy non-neoplastic urothelial cells, indicating the build-up of accentuated autophagosome (mitophagosome) formation in urothelial cancer cells under hypoxia stresses (Fig. 6). Ultrastructural findings appeared to corroborate these mechanistic molecular features. Indeed, phagophore membranes were observed, some of which expanded and appeared to selectively sequester damaged mitochondria in a double membrane-bound mitophagosome appearance (Fig. 7). No phagophore membranes were seen in healthy, non-neoplastic urothelial cells. Together, molecular and ultrastructural findings of our study provide evidence that FUNDC1-mediated mitophagy is activated in urothelial cells infected by BPVs.

3.3. Mitochondrial DRP1 translocation and activation

It has been proposed that FUNDC1 is specifically required for mitochondrial fission as it recruits and creates a direct physical association with DRP1, a cytosolic mechanoenzyme believed to be the central player in the fission events of mitochondrial dynamics (Wu et al., 2016; Chen and Chan, 2017). Therefore, we wanted to investigate whether FUNDC1 was responsible for mitochondrial recruitment of DRP1, and whether FUNDC1/DRP1 complex was a mechanistic event in bovine urothelial cells. First, we carried out western blot analysis on total extracts and found statistically significant overexpression of the mechanoenzyme in urothelial cancer cells (Fig. 8). Furthermore, we detected DRP1 expression in mitochondrial, cytosolic, and microsomal fractions of neoplastic and non-neoplastic cells. DRP1 appeared to show statistically significant increase at the mitochondrial level in neoplastic cells (Fig. 8). Next, we studied the DRP1 phosphorylation status, as DRP1 phosphorylation at serine 616 (Ser^{616}) is responsible for

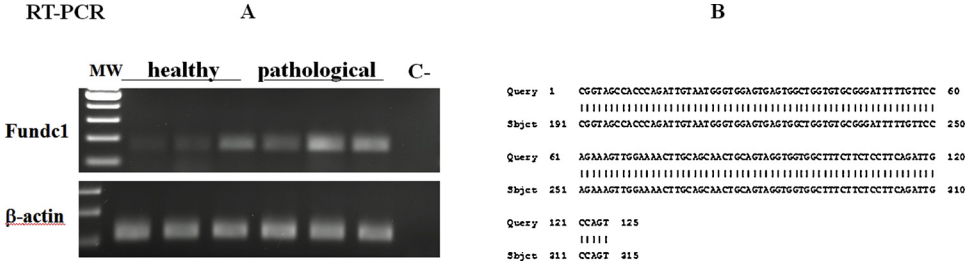

Fig. 3. (A): electrophoresis of RT-PCR products for analysis of FUNDC1 mRNA expression in healthy and pathological bovine bladder. MW: molecular weight marker (100-bp ladder); lanes 1-3: healthy urothelium samples; lanes 4-6: three representative urothelial endoluminal cancers; lane C-: PCR negative control. (B): Alignment of the sequences shows 100% identity with *Bos taurus* FUN14 domain containing 1 (FUNDC1) mRNA (accession number: NM_001104982).

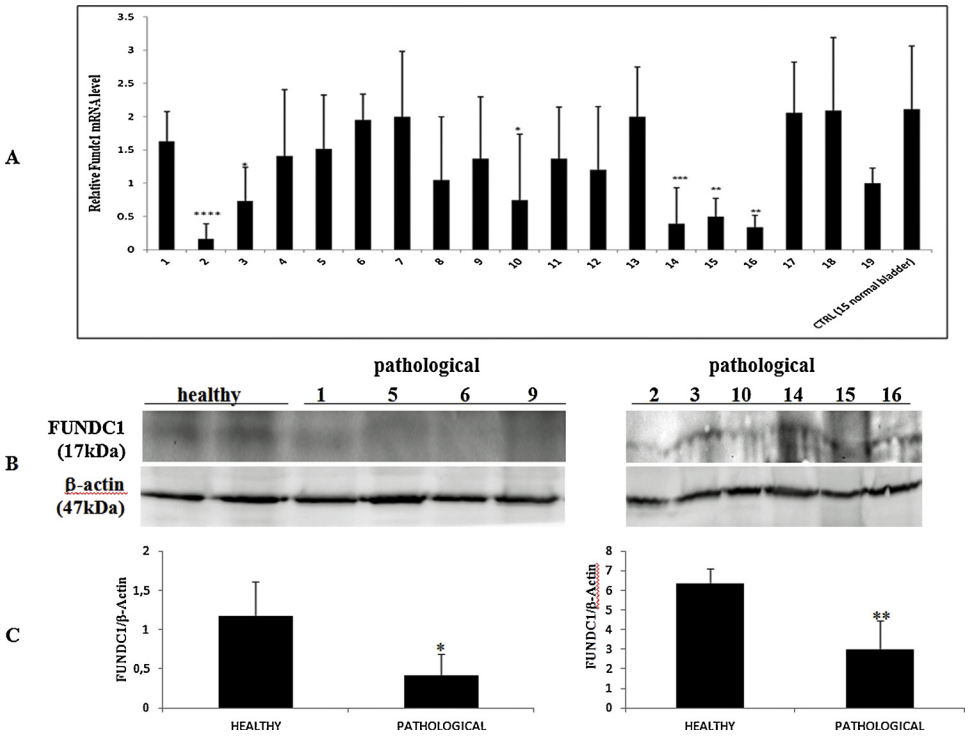

Fig. 4. (A) Real time RT-PCR: FUNDC1 mRNA levels in 15 normal control (CTRL) and 19 neoplastic bladder samples. In particular, it was shown that, in six bladder samples (No. 2, 3, 10, 14, 15, and 16), there was significant difference in the expression of FUNDC1 mRNA compared with normal bladders (*p ≤ 0.05). Data are expressed as mean ± S.E.M. of three separate experiments performed in triplicate (* p < 0.05; **p < 0.01; ***p < 0.001; **** p < 0.0001). (B) FUNDC1 western blot analysis on healthy and neoplastic urothelial cells. Lanes marked as "healthy": bladder samples from healthy cows; lanes marked with No. 1, 5, 6 and 9: neoplastic samples with normal FUNDC1 transcript levels; lanes marked as No. 2, 3, 10, 14, 15, and 16: neoplastic samples with reduced levels of FUNDC1 mRNA. (C) Densitometric analysis detecting statistically significant reduction of FUNDC1 protein levels in the neoplastic cells (* p < 0.05, **p < 0.01).

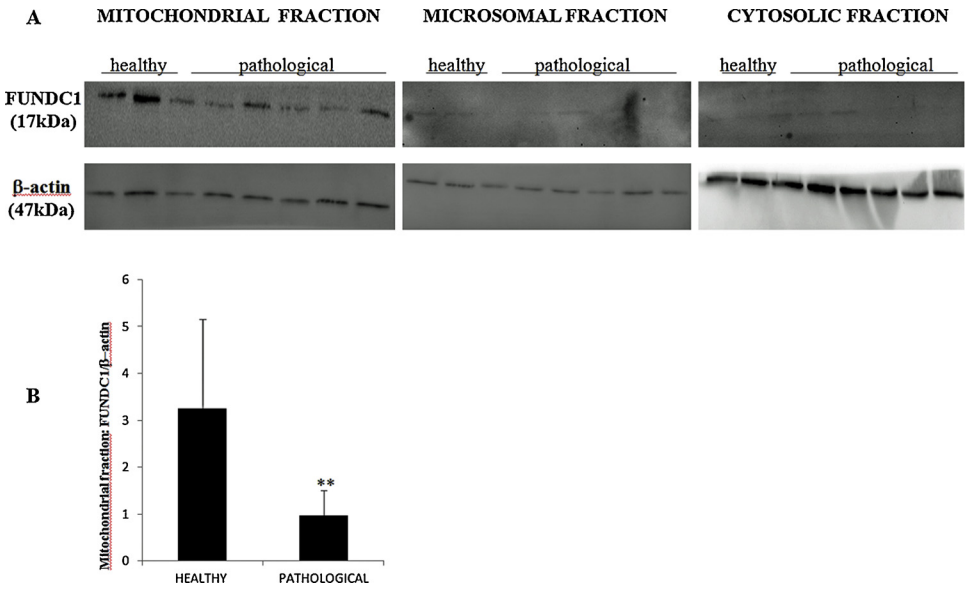

Fig. 5. (A) Western blot analysis of FUNDC1 in subcellular fractions (mitochondrial, microsomal, and cytosolic fractions). Ten micrograms of different subcellular protein fractions from healthy and neoplastic samples were electrophoresed through a denaturing polyacrylamide gel, electroblotted, and hybridised with anti-FUNDC1 or anti-β-actin antibody (as a loading control). (B) Densitometric analysis for FUNDC1 of mitochondrial fraction was performed in comparison with β-actin protein levels. The calculations were based on three independent determinations. The values for the latter are expressed as a percentage of the average values for the healthy samples (**p < 0.01).

fragmentation of the mitochondrial network. Indeed, phosphorylation at Ser^{616} increases Mff-dependent mitochondrial DRP1 recruitment and subsequent fission (Chen and Chan, 2017). We found that the phosphorylated form of DRP1 Ser^{616} was significantly increased in neoplastic cells, which suggested that mitochondrial fission, a pre-requisite for mitophagy, may be enhanced in cancer cells infected by bovine papillomavirus via phosphorylation of this enzyme (Fig. 8). Finally, we immunoprecipitated the mitochondrial fraction with an anti-FUNDC1 antibody and detected the DRP1 expression. This interaction was more evident in neoplastic cells infected by BPVs rather than in non-neoplastic urothelial cells (Fig. 6), which showed that DRP1 was recruited at the mitochondrial level and was a physical partner of FUNDC1.

3.4. DRP1 adaptors

DRP1 is known to translocate to fission sites of mitochondria through several receptors, including Mff, which represents a major and best-studied regulator of mitochondrial fission (Chen and Chan, 2017), Fis1, MiD49, and MiD51. As it is shown that phosphorylation of Mff is accompanied by a rise in DRP1 levels on the mitochondrial surface and subsequent fission (Rodger et al., 2018), we, first, investigated the Mff expression in mitochondrial, cytosolic, and microsomal subcellular fractions of neoplastic and healthy non-neoplastic cells. Mff expression in both total and phosphorylated components showed statistically significant increase at the mitochondrial level in neoplastic cells infected by bovine papillomavirus relative to healthy non-neoplastic urothelial cells (Fig. 9). Therefore, Mff overexpression and its increased phosphorylation were deemed responsible for its crucial role as an adaptor

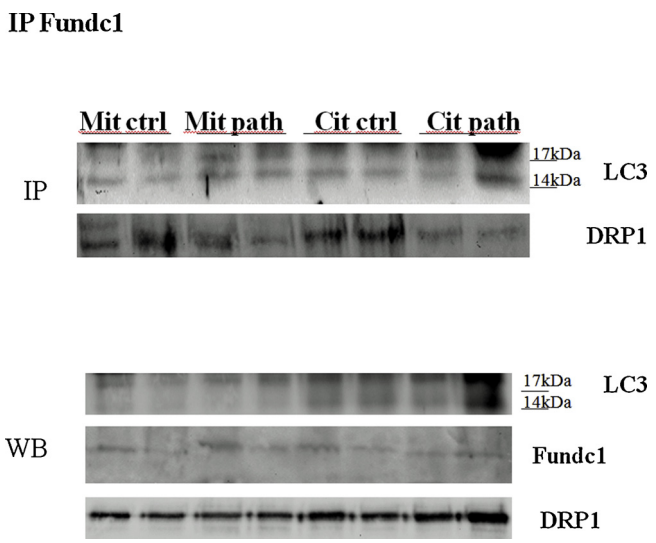

Fig. 6. FUNDC1 mitochondrion and cytosolic immunoprecipitation in non-neoplastic and neoplastic bladder samples. Western blot analysis revealed the presence of LC3 and DRP1 protein in anti-FUNDC1 immunoprecipitates.

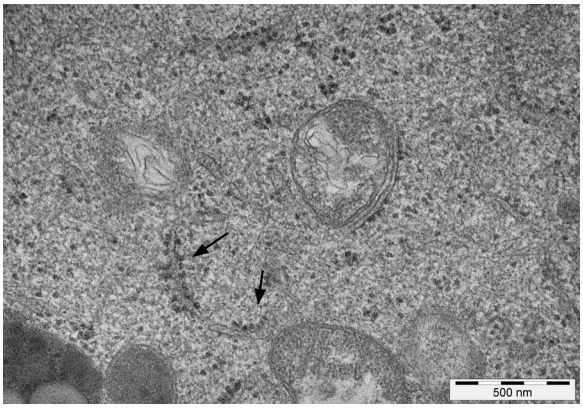

Fig. 7. A severely damaged mitochondrion delimited by phagophore that is expanding is shown. Free phagophores in expansion are also seen (arrows).

for mitochondrial recruitment of DRP1 in a spontaneous model of disease by papillomavirus infection, which resulted in an increased rate of fission. Furthermore, we detected significantly stronger mitochondrial expression of Fis1, MiD49, and MiD51 receptors in neoplastic urothelial cells than in healthy non-neoplastic cells (Fig. 10). All the receptors showed a very weak immunosignal in cytosolic and microsomal fractions. Although the role of Fis1 and MiD49/51 in mitochondrial fission is still controversial (Wu et al., 2016), it is highly likely that all the adaptors are involved, directly and/or indirectly, in the mitochondrial fission of urothelial cells infected by BPVs. Therefore, it is conceivable that mitochondrial fragmentation characterising the ultrastructural pattern of papillomavirus-associated urothelial cancer cells, may reflect fission events caused by phosphorylated DRP1 recruited by FUNDC1, and that phosphorylated Mff adaptor could enhance the translocation of DRP1 to mitochondria.

3.5. Bag3, Hsc70/Hsp70, CHIP and Synpo2 mitochondrial localization and interaction

Recently, Bag3 and Hsc70/Hsp70 have been ascribed a likely role in Parkin-dependent mitophagy (Tahrir et al., 2017; Zheng et al., 2018). Emerging evidence supports the mechanistic insights that these cytosolic proteins can be recruited to mitochondria (Tahrir et al., 2017; Li et al., 2019).

We wanted to test whether Bag3 co-chaperone could be localised at the mitochondrial level and potentially involved in mitophagy in our samples. Therefore, we performed western blot analysis, and detected Bag3 in all subcellular fractions, including mitochondria (Fig. 11). Furthermore, Bag3 was significantly overexpressed in the mitochondrial subcellular fraction of neoplastic cells relative to non-neoplastic cells (Fig. 11). Next, we carried out immunoprecipitation of mitochondrial subcellular fractions with an anti-Bag3 antibody, and detected, for the first time, through western blot analysis, the presence of both FUNDC1 and Hpc70/Hsp70, which suggested that Bag3 and its chaperone interact with FUNDC1 (Fig. 12). Indeed, CHIP is an HSC70-interacting E3 ubiquitin ligase that promotes the ubiquitination and subsequent degradation of HSC70 clients. Within the mitochondrial immunoprecipitates obtained with Bag3, we also detected also the presence of CHIP by western blot (Fig. 12). These data suggested that a complex composed of Bag3/Hsc70/Hsp70/CHIP is also present at the mitochondrial level. By analogy with the general autophagy machinery, Bag3, in association with Hsc70/Hsp70, may contribute to the transport of CHIP-ubiquitinated cargo. Very recently, it was experimentally shown that FUNDC1 interacts with Hsc70 and promotes the mitochondrial recruitment of the cargo clients, thus, contributing to their clearance and organisation of cellular proteostatic responses (Li et al., 2019). In line with these experimental studies, we speculated that FUNDC1 may be involved in a selective removal of the cargoes translocated to mitochondrial membrane by Hsc70/Hsp70 during spontaneous diseases by papillomavirus infection.

It has been suggested that interactions between Bag3 and synaptopodin 2 (Synpo2), a cytoskeleton adaptor protein that acts as a tumour suppressor in the bladder, play a crucial role for autophagosome formation in mechanically strained cells during general autophagy. To explore whether similar potential cooperation occurred during the mitophagy in bovine bladder, we investigated the mitochondrial immunoprecipitates obtained with Bag3, and detected the presence, of Synpo2 by western blot (Fig. 12). Taken together, these molecular findings are consistent with the assumption that Bag3 and Synpo2 are further involved in the formation of mitophagosome membrane during mitophagy.

4. Discussion

This study described FUNDC1-mediated mitophagy induced by hypoxia in a spontaneous model of disease by bovine papillomavirus in veterinary pathology. To our knowledge, this is the first report providing mechanistic insights into the mitophagy mediated by FUNDC1 in spontaneous viral infection in veterinary comparative medicine, which strengthens the statement that our knowledge on the role(s) of autophagy, including mitophagy, is still very limited in animal health and disease.

FUNDC1 basal expression occurred in healthy bovine urothelial cells, demonstrating that FUNDC1 was active in physiological contexts. It is conceivable that, as shown in other mammalian cells (Li et al., 2019), FUNDC1 may play a role in cellular proteostasis in bovine urothelial cells. Molecular and ultrastructural findings of this study showed that FUNDC1-mediated mitophagy was upregulated in hypoxic urothelial cancer cells of cattle infected by bovine papillomavirus.

We observed that both transcript and protein levels of FUNDC1 were decreased in neoplastic cells. Our molecular findings are consistent with previous experimental studies, which reported that FUNDC1 is down-regulated during hypoxia-induced mitophagy (Liu et al., 2012; Wei et al., 2015). Furthermore, we found that LC3 was present in the co-immunoprecipitates obtained with anti-FUNDC1 antibody, demonstrating that FUNDC1 interacts with this protein, an ultrastructural marker of autophagy, that is involved in autophagosome biogenesis. It has been shown that FUNDC1 initiates mitophagy in mammalian cells through its LIR (Chen et al., 2016; Liu et al., 2012). Ultrastructural findings of this study were characterised by the presence

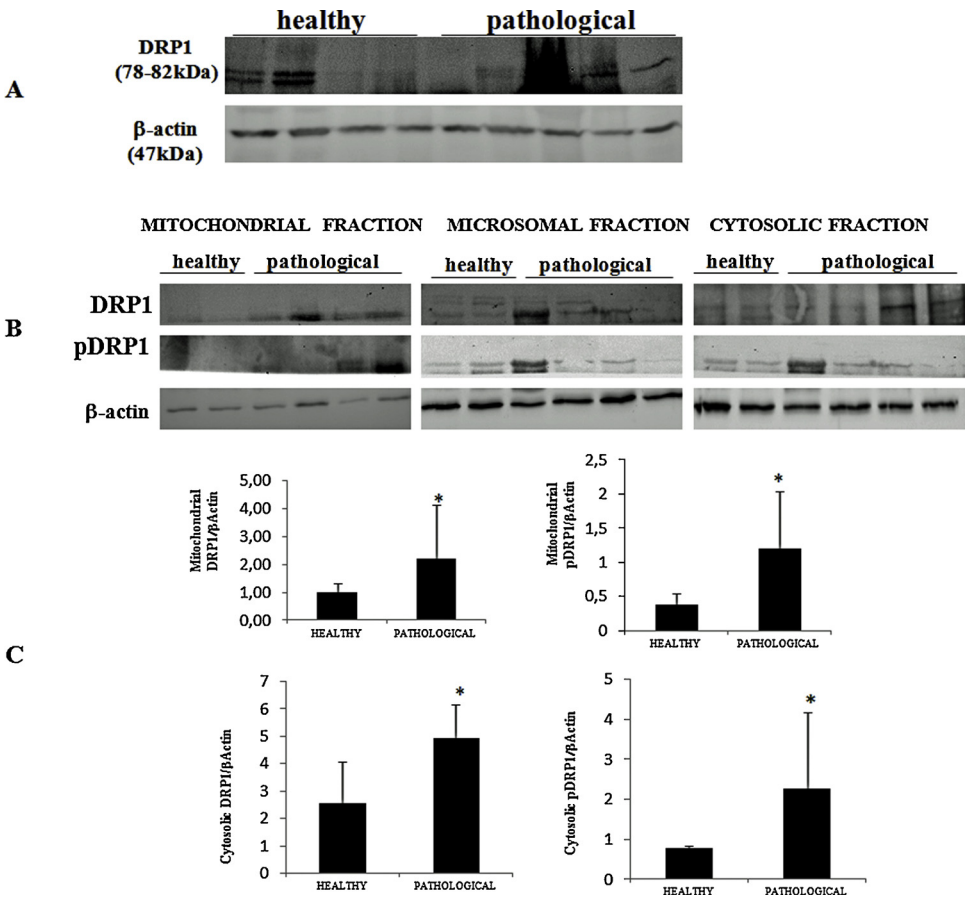

Fig. 8. Western blot analysis of DRP1 in the total lysate and DRP1 and pDRP1 in the subcellular fractions of healthy and neoplastic samples. (A) expression of DRP1 in total lysate; (B) subcellular fractions (mitochondrial, microsomal, and cytosolic fractions): 10 µg of different subcellular protein fraction was hybridised with anti-DRP1, anti-pDRP1 (Ser^{616}), or anti-βactin antibody (as a loading control). (C) densitometric analysis for mitochondrial and cytosolic DRP1 and pDRP1 was performed in comparison with β-actin protein levels. The calculations were based on three independent determinations. The values for the latter are expressed as a percentage of the average values for the healthy samples (*$p < 0.05$).

of numerous mitochondrion-sequestering autophagosomes (mitophagosomes) and autolysosomes. Furthermore, ultrastructural examination showed the existence of membrane contact between mitochondria and endoplasmic reticulum (ER). This submicroscopic pattern is consistent with the so-called mitochondrion-associated membrane (MAM), which is a functional "communication zones" (Shimizu, 2019). These zones, which are vital for organelle function, are also known as "mitophagy zones" as they could represent the starting point for mitophagy marked by the formation of autophagic membranes (Shimizu, 2019).

It has been shown that FUNDC1 regulates mitochondrial dynamics (Palikaras et al., 2018). FUNDC1 binds to DRP1, which leads to mitochondrial fission, and ultimately mitophagy (Chen et al., 2016; Wu

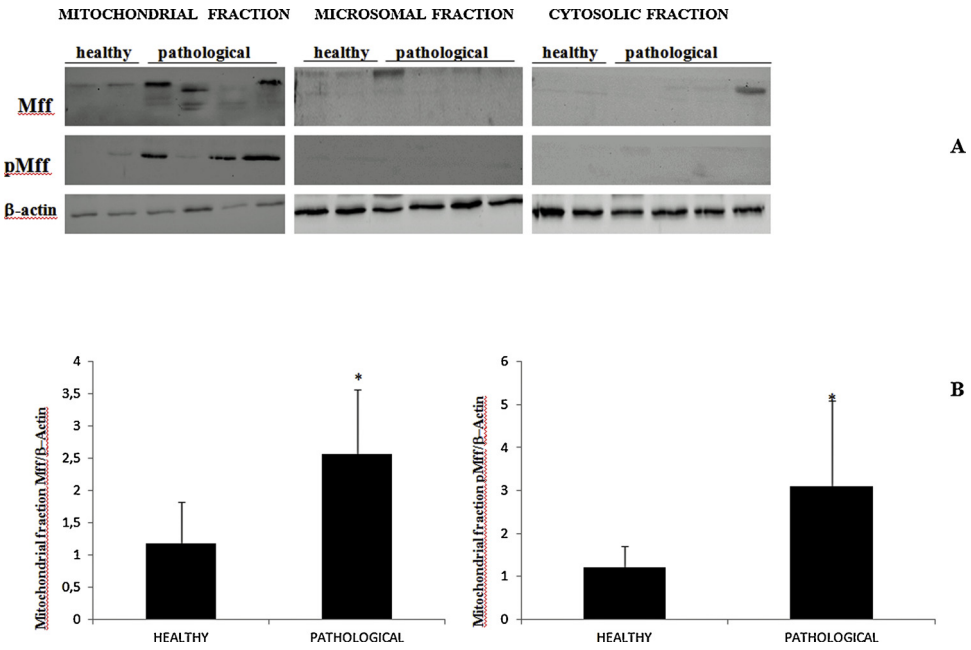

Fig. 9. (A) Western blot analysis of Mff and pMff in subcellular (mitochondrial, microsomal, and cytosolic) fractions of healthy and neoplastic samples. (B) Densitometric analysis for Mff and pMff proteins of the mitochondrial fraction was performed in comparison with β-actin protein levels (*$p < 0.05$).

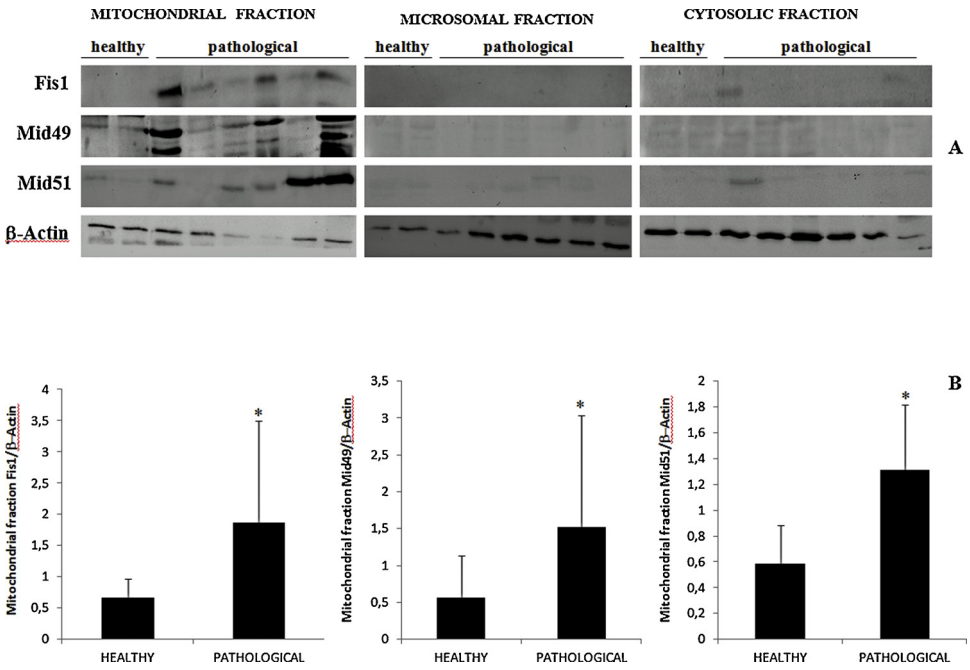

Fig. 10. (A) Western blot analysis of Fis1, MiD49, and MiD51in subcellular (mitochondrial, microsomal, and cytosolic) fractions of healthy and neoplastic samples. (B) Densitometric analysis for Fis1, MiD49, and MiD51 of the mitochondrial fraction was performed in comparison with β-actin protein levels (*$p < 0.05$).

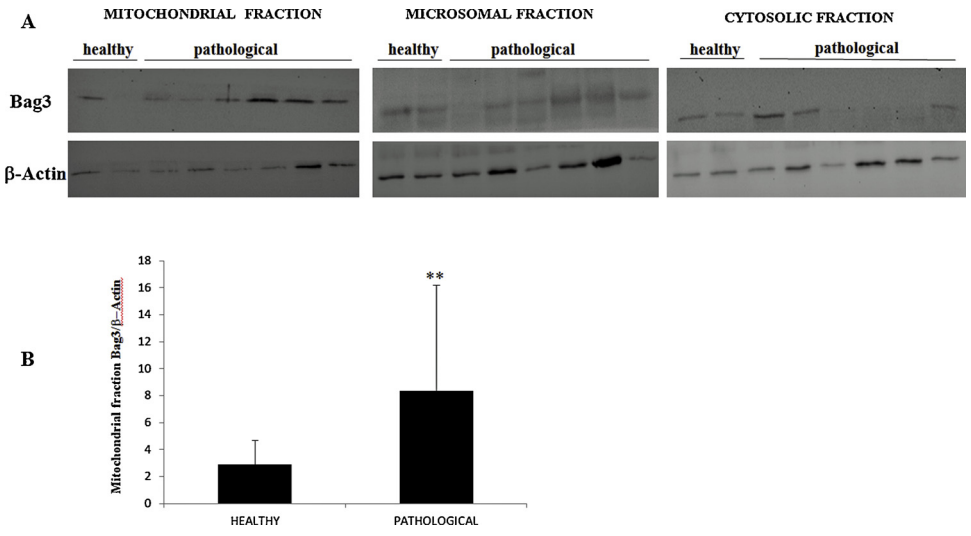

Fig. 11. (A) Western blot analysis of Bag3 in subcellular (mitochondrial, microsomal, and cytosolic) fractions of healthy and neoplastic samples. Ten μg of different subcellular protein fraction were hybridised with anti-Bag3 or anti-β-actin antibody as a loading control. (B) Densitometric analysis for Bag3 protein of the mitochondrial fraction was performed in comparison with β-actin protein levels. The calculations were based on three independent determinations. The values for the latter are expressed as a percentage of the average values for the healthy samples (**$p < 0.05$).

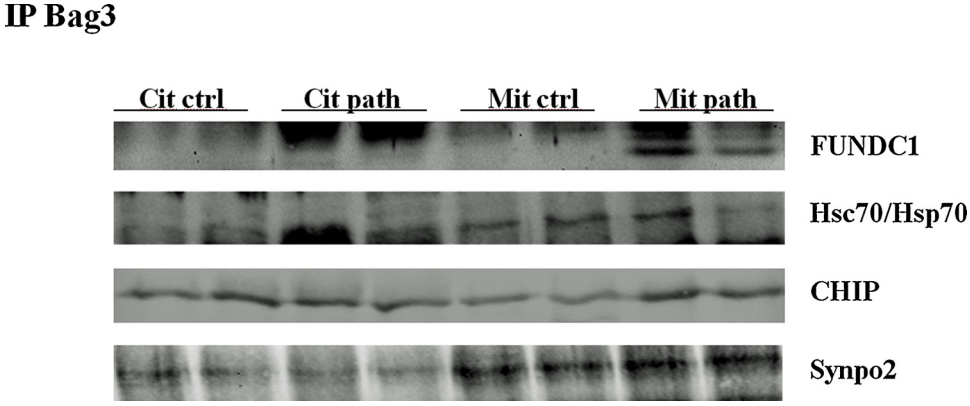

Fig. 12. Bag3 mitochondrial and cytosolic immunoprecipitation in non-neoplastic and neoplastic bladder samples. Western blot analysis revealed the presence of FUNDC1, Hsc70/Hsp70, CHIP, and Synpo2 proteins in anti-Bag3 immunoprecipitates.

et al., 2016). It is conceivable that FUNDC1 plays a central role in mitochondrion fragmentation via phosphorylated DRP1 as observed in our study. Indeed, it has been proposed that the functional properties of DRP1 rely on its phosphorylation status, which is essential for its interaction with phosphorylated Mff. This interaction activates DRP1 GPTase activity (Chen and Chan, 2017).

Very recently, it was demonstrated, for the first time, that Bag3 promotes Parkin-dependent mitophagy, which is critical for mitochondrial quality control (Tahrir et al., 2017).

Here, we showed that FUNDC1 was a partner of Bag3 and CHIP co-chaperones, as well as Hsc70/Hsp70 chaperone. Therefore, it is conceivable that Bag3 may also play an important role as mitophagy receptor in the papillomavirus-associated urothelial cancer cells of cattle. Our assumption is strengthened by the presence of FUNDC1 and Hsc70/Hsp70 in mitochondrial fractions of urothelial cancer cells immunoprecipitated by Bag3. As FUNDC1/Hsc70/Hsp70 interaction promotes mitochondrial translocation of unwanted cytosolic protein (Li et al., 2019), it is conceivable that Bag3, at the mitochondrial level, may play a role in transporting Hsc70/Hsp70-bound CHIP-ubiquitinated substrate for degradation. It is well known that Bag3 supports autophagosome formation by interacting with Synpo2 in general autophagy (Stürner and Behl, 2017). Therefore, the Bag3/Synpo2 complex detected at mitochondrial level allows us to suggest that Bag3 may be involved in mitophagosome biogenesis.

Several studies have suggested that viruses trigger mitophagy to promote viral replication (Zhang et al., 2018). Productive infection resulting in viral replication has been shown to occur in bovine papillomavirus-associated diseases of cattle (Roperto et al., 2013a). Although studies reporting organelle dynamics in the face of viral infections are scarce (Glingston et al., 2019), it is reasonable to speculate that BPV E5 oncoprotein could play a role in the mitophagy of naturally occurring bladder cancer in cattle. It is worth noting that BPV E5 oncoprotein has been shown to be involved in general autophagy mediated by Bag3 (Roperto et al., 2018).

Although the roles of FUNDC1 during virus infections and in cancer biology remain unknown, it has been suggested that FUNDC1 expression correlates negatively with the prognosis of human cancer caused by high-risk papillomaviruses (Hou et al., 2017). Recent studies revealed that biological behaviour of tumours may rely on FUNDC1 as it has been shown that overexpression of FUNDC1 promotes breast cancer proliferation and migration (Wu et al., 2019).

It is conceivable that activation of autophagy in general, and mitophagy in particular, may be involved in modulating the biological behaviour of papillomavirus-associated urothelial cancers of cattle characterised by a relatively low percentage of metastasis (8%–10%) (Pamukcu, 1974; Roperto et al., 2010a). Our suggestions are corroborated by recent experimental studies, which showed, for the first time, that HPV early protein 7 (E7) enhances ceramide-mediated mitophagy, thus, inducing tumour suppression (Thomas et al., 2017).

Of note, it has been suggested that an improved autophagy during viral infections correlates negatively with tumour development whereas impairment of the autophagy and mitophagy machinery promotes progression to metastasis in many malignancies, including the malignancies associated with HPVs (Mattoscio et al., 2018).

5. Conclusion

Mitophagy is an emerging research area for both fundamental discovery and therapeutic applications. To date, the lack of robust methods to assess in vivo mitophagy has hampered progress in determining the precise role of mitophagy in normal physiology and various disease states (Sun et al., 2015). Further in-depth studies in healthy and diseased domestic animals, which may serve as spontaneous model of disease, are warranted as they could provide useful insights into this specific field, a burgeoning area of research, as well as the development of novel therapeutic protocols.

Declaration of conflicting interests

The author(s) declared no potential conflicts of interests with respect to the research, authorship, and/or publication of this article.

Funding

The author(s) disclosed receipt of the following financial support for the research, authorship, and/or publication of this article: This research was partially supported by Regione Campania and Regione Basilicata. The funders of the work did not influence study design, data collection and analysis, decision to publish, or preparation of the manuscript.

Acknowledgements

We would like to thank prof. D. DiMaio, Yale University, New Haven, for kindly providing an anti-E5 rabbit polyclonal antiserum; Dr G. Salvatore, Regione Basilicata for his technical help.

Appendix A. Supplementary data

Supplementary material related to this article can be found, in the online version, at doi:https://doi.org/10.1016/j.vetmic.2019.05.017.

References

Chen, H., Chan, D.C., 2017. Mitochondrial dynamics in regulating the unique phenotypes of cancer and stem cells. Cell Metab. 26, 39–48.
Chen, M., Chen, Z., Wang, Y., Tan, Z., Zhu, C., Li, Y., Han, Z., Chen, L., Gao, R., Liu, L., Chen, Q., 2016. Mitophagy receptor FUNDC1 regulates mitochondrial dynamics and mitophagy. Autophagy 12, 689–702.
Daskalaki, I., Gkikas, I., Tavernarakis, N., 2018. Hypoxia and selective autophagy in cancer development and therapy. Front. Cell Dev. Biol. 6, 104. https://doi.org/10.3389/fcell.2018.00104.
Daudt, C., Da Silva, F.R.C., Lunardi, M., Alves, C.B.D.T., Weber, M.N., Cibulski, S.P., Alfieri, A.F., Alfieri, A.A., Canal, C.W., 2018. Papillomavirus in ruminants: an update. Transbound. Emerg. Dis. 65, 1381–1395.
DiMaio, D., Petti, L., 2013. The E5 proteins. Virology 445, 99–114.
Glingston, R.S., Deb, R., Kumar, S., Nagotu, S., 2019. Organelle dynamics and viral infections: at cross roads. Microbes Infect. 21, 20–32.
Guo, Y., Meng, X., Ma, J., Zheng, Y., Wang, Q., Wang, Y., Shang, H., 2014. Human papillomavirus 16 E6 contributes HIF-1α induced Warburg effect by attenuating the VHL- HIF-1α interaction. Int. J. Mol. Sci. 15, 7974–7986.
Hamacher-Brady, A., Brady, N.R., 2016. Mitophagy programs: mechanisms and physiological implications of mitochondrial targeting by autophagy. Cell. Mol. Life Sci. 73, 775–795.
Hou, H., Er, P., Cheng, J., Chen, X., Ding, X., Wang, Y., Chen, X., Yuan, Z., Pang, Q., Wang, P., Qian, D., 2017. High expression of FUNDC1 predicts poor prognostic outcomes and is a promising target to improve chemoradiotherapy effects in patients with cervical cancer. Cancer Med. 6, 1871–1881.
Li, Y., Xue, Y., Xu, X., Wang, G., Liu, Y., Wu, H., Li, W., Wang, Y., Ziheng, C., Zhang, W., Zhu, Y., Ji, W., Xu, T., Liu, L., Chen, Q., 2019. A mitochondrial FUNDC1/HSC70 interaction organizes the proteostatic stress response at the risk of cell morbidity. EMBO J. 38, e98786. https://doi.org/10.15252/embj.201798786.
Ling, Y., Zhang, X., Qi, G., Yang, S., Jingjiao, L., Shen, Q., Wang, X., Cui, L., Hua, X., Deng, X., Delwart, E., Zhang, W., 2019. Viral metagenomics reveals significant viruses in the genital tract of apparently healthy dairy cows. Arch. Virol. 164, 1059–1167.
Liu, L., Feng, D., Chen, G., Chen, M., Zheng, Q., Song, P., Ma, Q., Zhu, C., Wang, R., Qi, W., Huang, L., Li, B., Wang, X., Jin, H., Wang, J., Yang, F., Liu, P., Zhu, Y., Sui, S., Chen, Q., 2012. Mitochondrial outer-membrane protein FUNDC1 mediates hypoxia-induced mitophagy in mammalian cells. Nat. Cell Biol. 14, 177–186.
Liu, L., Sakakibara, K., Chen, Q., Okamoto, K., 2014. Receptor-mediated mitophagy in yeast and mammalian systems. Cell Res. 24, 787–795.
Masoud, G.N., Li, W., 2015. HIF-1α pathway: role, regulation and intervention for cancer therapy. Acta Pharm. Sin. B 5, 378–389.
Mattoscio, D., Medda, A., Chiocca, S., 2018. Human papilloma virus and autophagy. Int. J. Mol. Sci. 19, 1775. https://doi.org/10.3390/ijms19061775.
Palikaras, K., Lionaki, E., Tavernarakis, N., 2018. Mechanisms of mitophagy in cellular homeostasis, physiology and pathology. Nat. Rev. Biol. 20, 1013–1022.
Pamukcu, A.M., 1974. Tumours of the urinary bladder. Bull. Wld. Hlth. Org. 50, 43–52.
Pickles, S., Vigié, P., Youle, R.J., 2018. Mitophagy and quality control mechanisms in mitochondrial maintenance. Curr. Biol. 28, R170–R185.
Rodger, C.E., McWilliams, T.G., Ganley, I.G., 2018. Mammalian mitophagy - from *in vitro* molecules to *in vivo* models. FEBS J. 285, 1185–1202.
Roperto, S., Borzacchiello, G., Brun, R., Leonardi, L., Maiolino, P., Martano, M., Paciello, O., Papparella, S., Restucci, B., Russo, V., Salvatore, G., Urraro, C., Roperto, F.,

2010a. A review of bovine urothelial tumours and tumour-like lesions of the urinary bladder. J. Comp. Pathol. 142, 95–108.
Roperto, S., Borzacchiello, G., Esposito, I., Riccardi, M., Urraro, C., Lucà, R., Corteggio, A., Tatè, R., Cermola, M., Paciello, O., Roperto, F., 2012. Productive infection of bovine papillomavirus type 2 in the placenta of pregnant cows affected with urinary bladder tumors. PLoS One 7 (3), e33569.
Roperto, S., Comazzi, S., Ciusani, E., Paolini, F., Borzacchiello, G., Esposito, I., Lucà, R., Russo, V., Urraro, C., Venuti, A., Roperto, F., 2011. PBMCs are additional sites of productive infection of bovine papillomavirus type 2. J. Gen. Virol. 92, 1787–1794.
Roperto, S., De Tullio, R., Raso, C., Stifanese, R., Russo, V., Gaspari, M., Borzacchiello, G., Averna, M., Paciello, O., Cuda, G., Roperto, F., 2010b. Calpain3 is expressed in a proteolytically active form in papillomavirus-associated urothelial tumors of the urinary bladder in cattle. PLoS One 5 (4), e10299.
Roperto, S., Russo, V., Borzacchiello, G., Urraro, C., Lucà, R., Esposito, I., Ricciardi, M.G., Raso, C., Gaspari, M., Ceccarelli, D.M., Galasso, R., Roperto, F., 2014. Bovine papillomavirus type 2 (BPV-2) E5 oncoprotein binds to the subunit D of the V_1-ATPase proton pump in naturally occurring urothelial tumors of the urinary bladder of cattle. PLoS One 9 (2), e88860.
Roperto, S., Russo, V., Leonardi, L., Martano, M., Corrado, F., Riccardi, M.G., Roperto, F., 2016. Bovine papillomavirus type 13 expression in the urothelial bladder tumours of cattle. Transbound. Emerg. Dis. 63, 628–634.
Roperto, S., Russo, V., Ozkul, A., Corteggio, A., Sepici-Dincel, A., Catoi, C., Esposito, I., Ricciardi, M.G., Urraro, C., Lucà, R., Ceccarelli, D.M., Longo, M., Roperto, F., 2013a. Productive infection of bovine papillomavirus type 2 in the urothelial cells of naturally occurring urinary bladder tumors in cattle and water buffaloes. PLoS One 8 (5), e62227.
Roperto, S., Russo, V., Ozkul, A., Sepici-Dincel, A., Maiolino, P., Borzacchiello, G., Marcus, I., Esposito, I., Riccardi, M.G., Roperto, F., 2013b. Bovine papillomavirus type 2 infects the urinary bladder of water buffalo (Bubalus bubalis) and plays a crucial role in bubaline urothelial cancerogenesis. J. Gen. Virol. 94, 403–408.
Roperto, S., Russo, V., Rosati, A., Ceccarelli, D.M., Munday, J.S., Turco, M.C., Roperto, F., 2018. Chaperone-assisted selective autophagy in healthy and papillomavirus-associated neoplastic urothelium of cattle. Vet. Microbiol. 221, 134–142.
Shimizu, S., 2019. Organelle zones in mitochondria. J. Biochem. 165, 101–107.
Stürner, E., Behl, C., 2017. The role of the multifunctional Bag3 protein in cellular protein quality control and disease. Front. Mol. Neurosci. 10, 177. https://doi.org/10.3389/fnmol.2017.00177.
Sun, N., Yun, J., Liu, J., Malide, D., Liu, C., Rovira, I.I., Holmström, K.M., Fergusson, M.M., Yoo, Y.H., Combs, C.A., Finkel, T., 2015. Measuring in vivo mitophagy. Mol. Cell 60, 685–696.
Tahrir, F.G., Knezevic, T., Gupta, M.K., Gordon, J., Cheung, J.Y., Feldman, A.M., Khalili, K., 2017. Evidence for the role of Bag3 in mitochondrial quality control in cardiomyocytes. J. Cell. Physiol. 232, 797–805.
Thomas, R.J., Oleinik, N., Selvam, S.P., Vaena, S.G., Dany, M., Nganga, R.N., Depalma, R., Baron, K.D., Kim, J., Szulc, Z.M., Ogretmen, B., 2017. HPV/E7 induces chemotherapy-mediated tumor suppression by ceramide-dependent mitophagy. EMBO Mol. Med. 9, 1030–1051.
Twig, G., Shirihai, O.S., 2011. The interplay between mitochondrial dynamics and mitophagy. Antioxid. Redox Signal. 14, 1939–1951.
Youle, R.J., Narendra, D.P., 2011. Mechanisms of mitophagy. Nat. Rev. Mol. Cell Biol. 12, 9–14.
Wei, H., Liu, L., Chen, Q., 2015. Selective removal of mitochondria via mitophagy: distinct pathways for different mitochondrial stresses. Biochim. Biophys. Acta 1853, 2784–2790.
Wu, W., Lin, C., Wu, K., Jiang, L., Wang, X., Li, W., Zhuang, H., Zhang, X., Chen, H., Li, S., Yang, Y., Lu, Y., Wang, J., Zhu, R., Zhang, L., Sui, S., Tan, N., Zhao, B., Zhang, J., Li, X., Feng, D., 2016. FUNDC1 regulates mitochondrial dynamics at the ER-mitochondrial contact site under hypoxic conditions. EMBO J. 35, 1368–1384.
Wu, L., Zhang, D., Zhou, L., Zhuang, Y., Cui, W., Chen, J., 2019. FUN14 domain-containing 1 promotes breast cancer proliferation and migration by activating calcium-NFATC1-BMI1 axis. EBioMedicine 41, 276–285.
Zhang, L., Quin, Y., Chen, M., 2018. Viral strategies for triggering and manipulating mitophagy. Autophagy 14, 1665–1673.
Zheng, Q., Huang, C., Guo, J., Tan, J., Wang, C., Tang, B., Zhang, H., 2018. Hsp70 partecipates in PINK1-mediated mitophagy by regulating the stability of PINK1. Neurosci. Lett. 662, 264–270.